

## Supplementary Materials

### Supplementary Methods

#### CRISPR/Cas9 library screening and sgRNA sequence

Supernatants containing the CRISPR/Cas9 lentiviral system were added to Fadu cells after 18 h of starvation. After infection for 48 h, 2.0  $\mu$ g/ml puromycin was added to the medium to select the infected cells. After additional 72 h, 1.0  $\mu$ g/ml of cisplatin was added to select genes contributing to cisplatin resistance as we mentioned in previous article(Miao et al., 2023).

#### In vivo experiments

The mice were monitored for weight, tumor growth, and general behavior. The mice were sacrificed after the experiment, and tumors and organs were surgically dissected. Immunohistochemistry (IHC) or immunofluorescence (IF) and TUNEL assays were performed on tumor sections.

#### Flow cytometry

An Annexin V-Propidium Iodide kit was used to determine the proportion of apoptotic cells in the control, shSREBF1, and shPIK3R3 groups following the manufacturer's instructions (Solarbio, Beijing, China).

#### GO function and pathway enrichment analyses of the differentially expressed sgRNAs

We performed differentially expressed sgRNA enrichment analyses using the R environment cluster profile (3.14RC2) and package “org.Hs.eg.db (3.10)” for GO function and pathway enrichment analyses of the differentially expressed sgRNAs from the CRISPR/Cas9 library screening. Differential analyses were conducted in the biological process (BP), cellular component (CC), and molecular function (MF) categories and for pathways. The BH method was used for multiple testing corrections.

#### EdU, live/dead, and TUNEL staining.

The cell proliferation assay was performed using a commercial EdU staining kit (kFluor488 Click-iT EdU Imaging Assay kit, KeyGen, Nanjing, Jiangsu, China) according to the manufacturer's instructions. EdU is incorporated into DNA during DNA synthesis. The live/dead cell distribution was examined using a commercial Live/Dead staining kit (Calcein/PI CELL Viability/Cytotoxicity Assay kit, KeyGen, Nanjing, Jiangsu, China) according to the manufacturer's instructions. 3D organoids were fixed with 4% paraformaldehyde and then permeabilized with ethanol to allow penetration of the TUNEL reaction reagents into the nuclei. Following fixation and washing, incorporation of biotinylated dUTP onto the 3' ends of fragmented DNA was performed with TdT. Following staining with fluorescent-tagged avidin, the incorporated biotinylated dUTP was visualized by fluorescence microscopy. Tissue sections were multi-stained with DAPI and analyzed by microscopy.

#### Lentivirus transfection with shRNA

Fadu cells were transfected with lentivirus particles of short hairpin RNA (shRNA) for SREBF1 or PIK3R3 and their corresponding negative controls (NC) (GenePharma, Shanghai, Shanghai, China). Supernatants containing lentivirus expressing shRNA were har

vested 18 h after transfection. After infection for 72 h, 2.0  $\mu$ g/ml puromycin was added to the medium to select the infected cells.

#### **RNA extraction and real-time PCR**

Total RNA was extracted from cell lines using TRIzol (TaKaRa, Dalian, Liaoning, China), and cDNA synthesis and reverse transcription were performed with the PrimeScript™ RT reagent kit (TaKaRa, Dalian, Liaoning, China). Gene expression values were normalized with  $\beta$ -actin (BBI, Shanghai, China) and compared with control samples. Primers and shRNA target sequence are listed as Table S3.

#### **Hematoxylin–eosin staining, immunohistochemistry, and immunofluorescence**

Paraformaldehyde-fixed organoids or samples were embedded in paraffin and cut into 4- $\mu$ m-thick sections. After Hematoxylin-eosin (HE) staining, another slice was then incubated first with primary antibody (anti-SREBF1, anti-PIK3R3, anti-CD44, anti-CD133) (Abcam, Boston, MA, USA) at 4°C overnight and then with secondary antibody for 2 h at room temperature. The sections were viewed using a Zeiss Zen 3.3 system and images were analyzed using Image J.

#### **Reference:**

Miao, X., Wang, H., Fan, C., Song, Q., Ding, R., Wu, J., Hu, H., Chen, K., Ji, P., Wen, Q., Shi, M., Ye, B., Fu, D., & Xiang, M. (2023). Enhancing prognostic accuracy in head and neck squamous cell carcinoma chemotherapy via a lipid metabolism-related clustered polygenic model. *Cancer Cell Int*, 23(1), 164.

<https://doi.org/10.1186/s12935-023-03014-5>

## Supplementary Table and Figures

**Table S1. Characteristics of TCGA HNSCC cohort.**

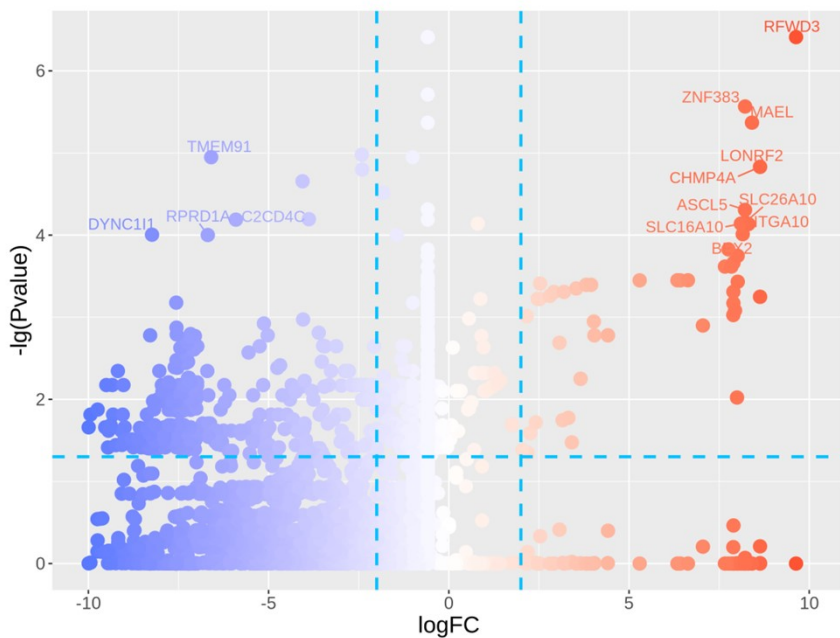
	LMRS-High group	LMRS-Low group
<b>Total</b>	<b>117</b>	<b>56</b>
<b>Gender</b>		
Female	26	8
Male	91	48
<b>Race</b>		
American Indian	1	0
Asian	5	0
Black	12	7
White	96	49
<b>Tumor</b>		
1	4	3
2	26	15
3	37	14
4	50	24
<b>Node</b>		
0	44	8
1	14	11
2	54	33
3	1	4
<b>Metastasis</b>		
No	112	53
Yes	2	0
<b>TNM Stage</b>		
1 <sup>st</sup>	2	0
2 <sup>nd</sup>	7	1
3 <sup>rd</sup>	14	7
4 <sup>th</sup>	94	48
<b>Histology Grade</b>		
Grade 1	5	3
Grade 2	77	32
Grade 3	27	13
Grade 4	1	1
<b>Treatment</b>		
Chemotherapy	109	50
Immunotherapy	0	2
Radiotherapy	43	18
Neoadjuvant	2	2
<b>Smoking</b>		
Non-taker	26	16
Taker	91	39
<b>Alcohol</b>		
Non-taker	26	9
Taker	90	46

**Table S2. Characteristics of clinical samples**

Characteristic	Sensitive	Resistance	P Value
<b>Number, n</b>	10	20	
<b>Gender, n (%)</b>			<b>1.000</b>
Male	10 (33%)	20 (67%)	
Female	0 (0%)	0 (0%)	
<b>Smoke, n (%)</b>			<b>0.008</b>
No	4 (40%)	0 (0%)	
Yes	6 (60%)	20 (100%)	
<b>Alcohol, n (%)</b>			<b>0.045</b>
No	7 (70%)	5 (25%)	
Yes	3 (30%)	15 (75%)	
<b>Weight, median (IQR)</b>	75 (62, 75)	67 (65.6, 74)	<b>0.219</b>
<b>BMI, mean <math>\pm</math> SD</b>	23.544 (21.765, 24.212)	23.128 (22.501, 24.102)	<b>0.947</b>
<b>Triglycerides, mmol/L, mean <math>\pm</math> SD</b>	2.25 (2.055, 2.6475)	1.05 (0.905, 1.4425)	<b>&lt; 0.001</b>
<b>Free fatty acid, mmol/L, mean <math>\pm</math> SD</b>	0.399 $\pm$ 0.093506	0.43176 $\pm$ 0.13347	<b>0.502</b>
<b>T stage, n (%)</b>			<b>0.861</b>
T2	2 (20%)	4 (20%)	
T3	7 (70%)	11 (55%)	
T4	1 (10%)	5 (25%)	
<b>N stage, n (%)</b>			<b>0.563</b>
N0	1 (10%)	4 (20%)	
N1	4 (40%)	4 (20%)	
N2	5 (50%)	12 (60%)	
<b>M Stage, n (%)</b>			<b>1.000</b>
M0	10 (33%)	20 (67%)	
M1	0 (0%)	0 (0%)	

**Table S3 Primers and shRNA target sequence for SREBF1 and PIK3R3**

Name	Sequence
SREBF1 Forward primer	CGGAACCACATCTTGGCAACA
SREBF1 Reverse primer	GCCGGTTGATAAGGCAGCTT
PIK3R3 Forwards primer	CGGTCGGGTTGGTCTTACA
PIK3R3 Reverse primer	CTGGTCTGCAGAGAGCGAAT
shSREBF1-1	CAACAAAGACATGCAGAACAA
shSREBF1-2	GGGTGTATACTGTGAGATCAA
shSREBF1-3	TGGGACAAACTGTGACATCAA
shPIK3R3-1	GGAGAAGAGTAAAGAGTATGA
shPIK3R3-2	GGGAATTAAGAATGAGGATGC
shPIK3R3-3	GCTAGTGCTCCATTACCAGCA

**Figure S1. CRISPR/cas9 screened DEGs for cisplatin resistance in Fadu.** DEGs in the Fadu vs Fadu-DDP groups, with the following default criteria: P value<0.05 and FDR<0.25.

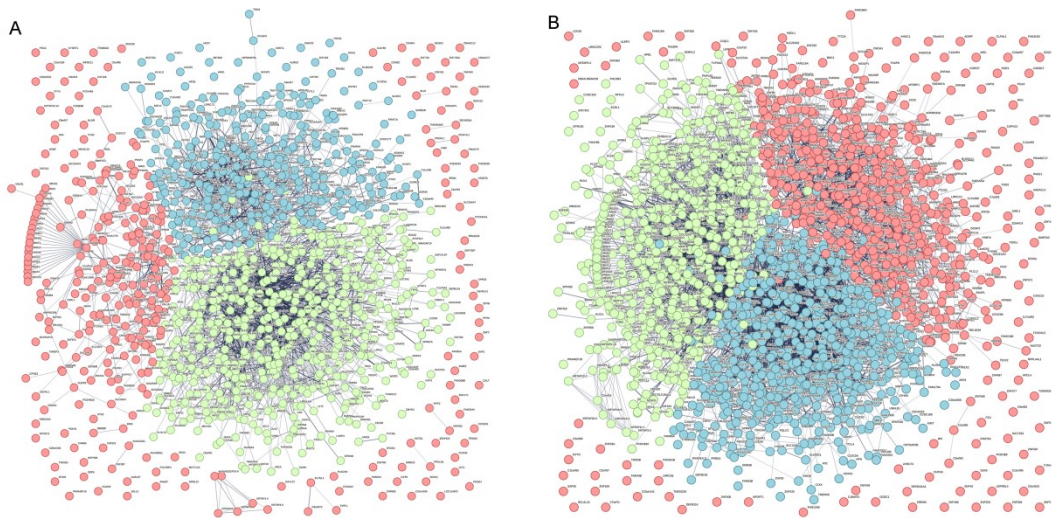


**Figure S2. Gene clusters for the CRISPR/cas9 screened DEGs. A** Gene clusters for the negative screened DEGs. **B** Gene clusters for the positive screened DEGs.

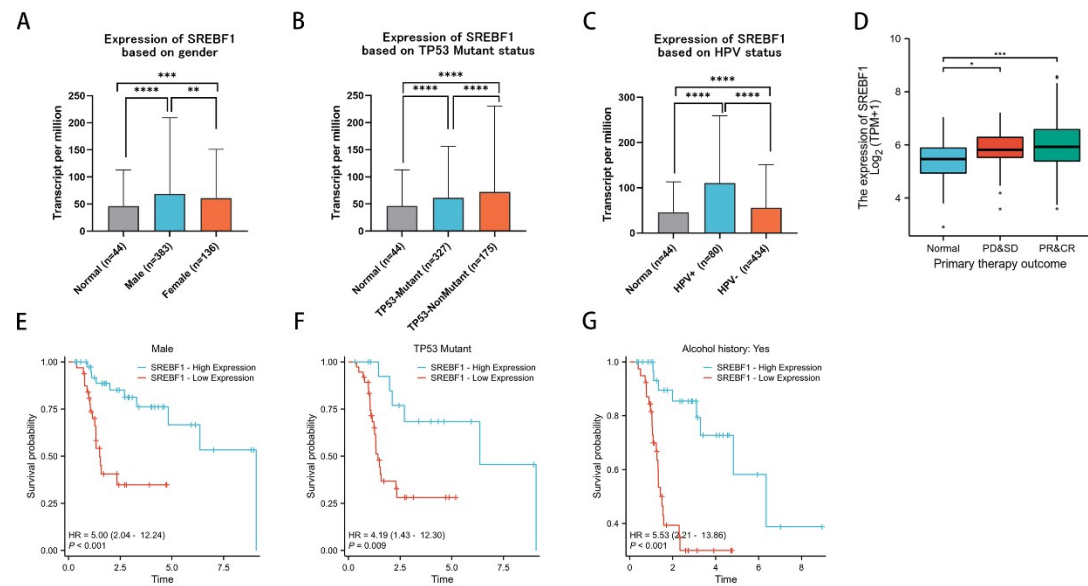


**Figure S3. Upregulated SREBF1 correlated with better prognosis and chemotherapy response in HNSCC patients. A.** Bar chart of the SREBF1 expression levels based on gender in TCGA-HNSCC cohort. **B.** Bar chart of the SREBF1 expression levels based on TP53 Mutant in TCGA-HNSCC cohort. **C.** Bar chart of the SREBF1 expression levels based on HPV status in TCGA-HNSCC cohort. **D.** Expression level of SREBF1 between normal, stable disease + progressive disease (SD+PD) and partial response +complete response (PR+CR). **E.** Kaplan-Meier survival analysis showed the Disease-free survival in SREBF1 high-expression group is better than the SREBF1 low-expression group in male group. **F.** Kaplan-Meier survival analysis showed the Disease-free survival in SREBF1 high-expression group is better than the SREBF1 low-expression group in male group in TP53 mutant group. **G.** Kaplan-Meier survival analysis showed the Disease-free survival in SREBF1 high-expression group is better than the SREBF1 low-expression group in male group in alcohol taker group.

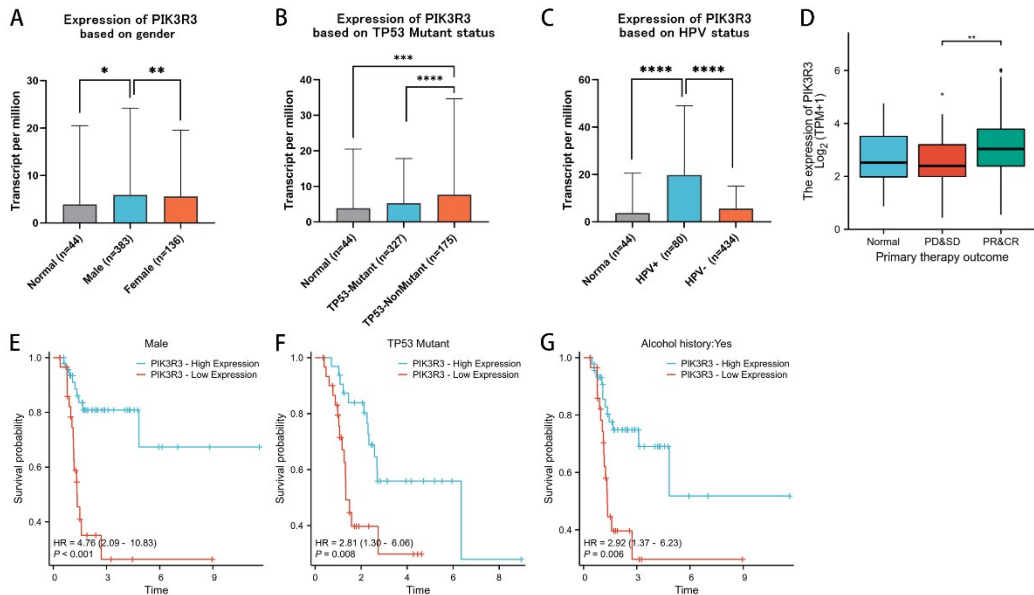


**Figure S4. PIK3R3 upregulation associated with improved prognosis and shared expression patterns with SREBF1 in HNSCC.** **A.** Bar chart of the SREBF1 expression levels based on gender in TCGA-HNSCC cohort. **B.** Bar chart of the SREBF1 expression levels based on TP53 Mutant in TCGA-HNSCC cohort. **C.** Bar chart of the SREBF1 expression levels based on HPV status in TCGA-HNSCC cohort. **D.** Expression level of SREBF1 between normal, stable disease + progressive disease (SD+PD) and partial response +complete response (PR+CR). **F.** Kaplan-Meier survival analysis showed the Disease-free survival in PIK3R3 high-expression group is better than the PIK3R3 low-expression group in male group in TP53 mutant group. **G.** Kaplan-Meier survival analysis showed the Disease-free survival in PIK3R3 high-expression group is better than the PIK3R3 low-expression group in male group in alcohol taker group.

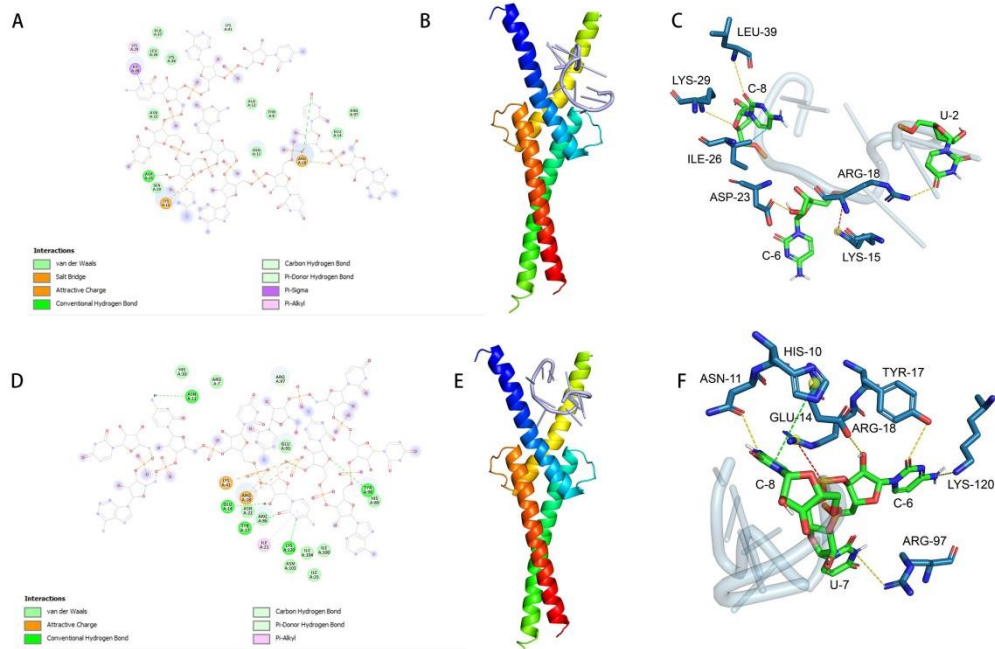


**Figure S5. PIK3R3 works as the downstream of SREBF1.** **A,B.** Visualization of molecular docking of SREBF1 to the PIK3R3 promoter region in structure 1 in 2D and 3D. **D, E.** Visualization of molecular docking of SREBF1 to the PIK3R3 promoter region in structure 2 in 2D and 3D. **C.** Visualization of molecular docking of SREBF1 to the *PIK3R3* promoter region in structure 1. **D.** Visualization of molecular docking of SREBF1 to the *PIK3R3* promoter region in structure 2. \* $P < 0.05$ , \*\* $P < 0.01$ , \*\*\* $P < 0.0001$ .

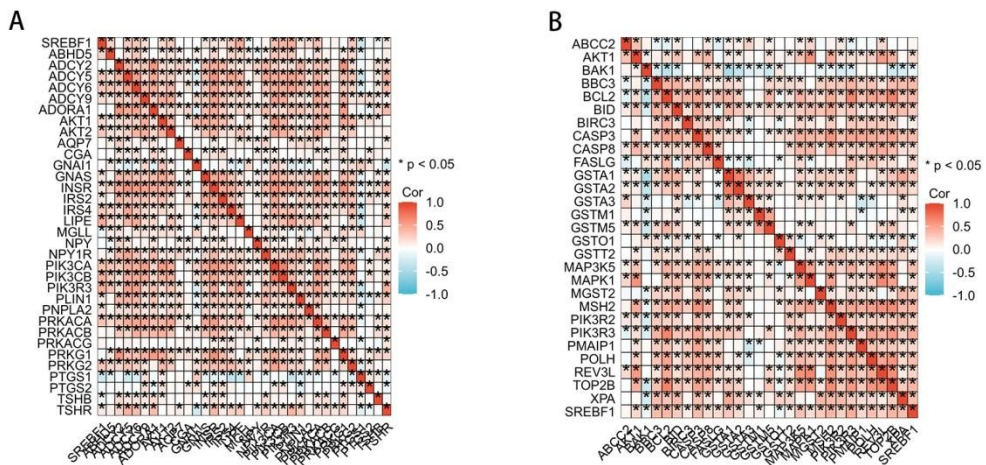


**Figure S6. PIK3R3 is associated with improved prognosis and shares patterns with SREBF1 in HNSCC.** (A) Heatmap of fatty acid metabolism genes co-expressed with SREBF1 (derived from the co-expression analysis). (B) Heatmap of drug metabolism genes co-expressed with SREBF1 (derived from the co-expression analysis). \* $P < 0.05$ , \*\* $P < 0.01$ , \*\*\* $P < 0.0001$ .

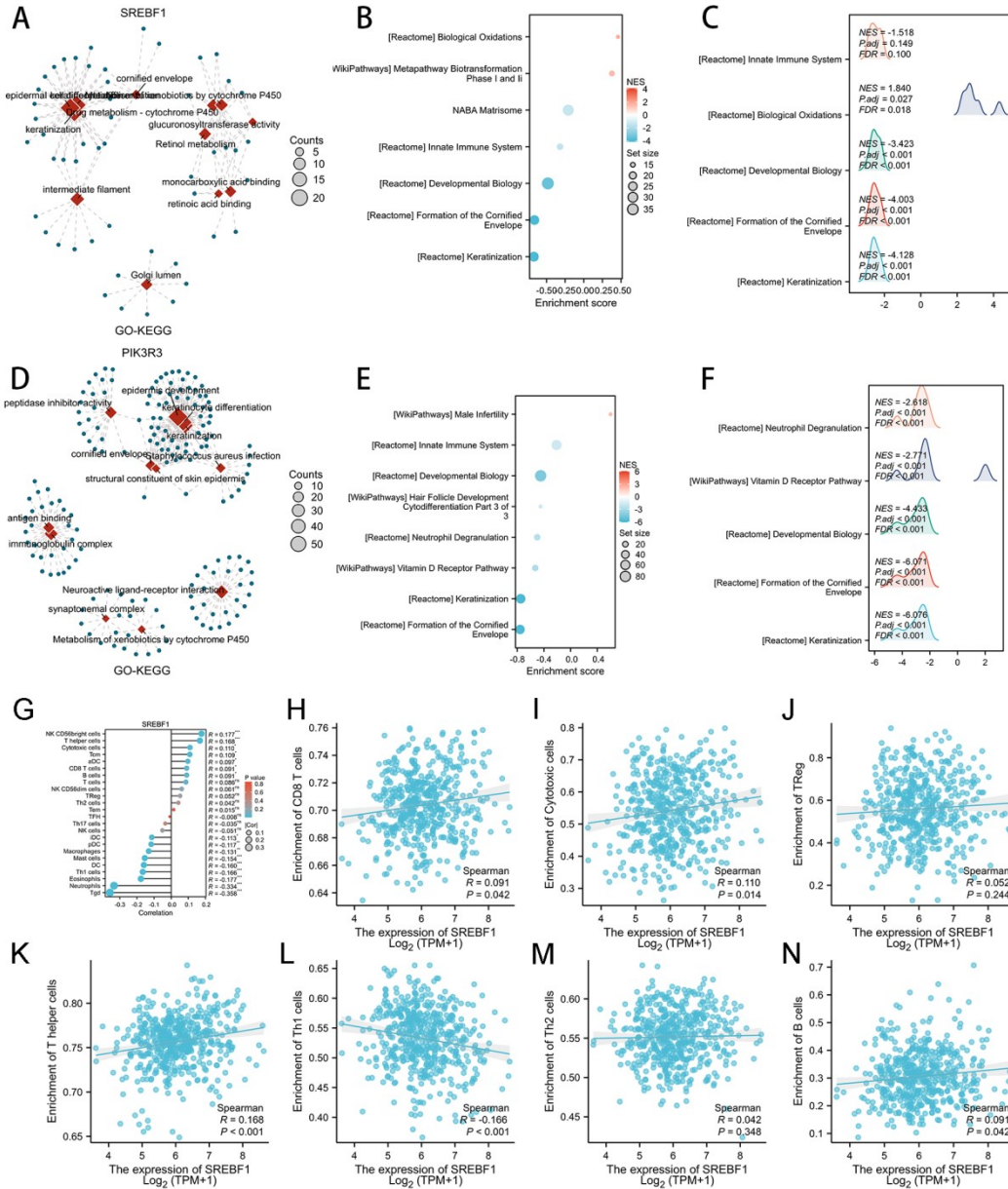


**Figure S7. The SREBF1/PIK3R3 axis affects tumor immunity in HNSCC.** (A) Chord diagram of GO functions and KEGG pathway enrichment analyses based on the DEGs from TCGA-HNSCC patients with different SREBF1 expression levels. (B) Bubble chart of the top enriched functions and pathways. Bubble size represents the number derived from different SREBF1 expression groups. (C) Genes enriched in representative pathways as determined by functional gene set enrichment analysis derived from different SREBF1 expression groups. (D) Chord diagram of GO functions and KEGG pathway enrichment analyses based on the DEGs from TCGA-HNSCC patients with different PIK3R3 expression levels. (E) Bubble chart of the top enriched functions and pathways. Bubble size represents the number derived from different PIK3R3 expression groups. (F) Genes enriched in representative pathways as determined by functional gene set enrichment analysis derived from different PIK3R3 expression groups. (G) Bubble plot representation showing the correlation between SREBF1 and 24 immune cells in the HNSCC samples of the TCGA cohort. (H) Scatter plot showing a positive correlation between CD8 T cell enrichment and the expression of SREBF1. (I) Scatter plot showing a positive correlation between cytotoxic T cell enrichment and the expression of SREBF1. (J) Scatter plot showing the correlation between regulatory T cell enrichment and the expression of SREBF1. (K) Scatter plot showing a positive correlation between T helper cell enrichment and the expression of SREBF1. (L) Scatter plot showing a negative correlation between T helper 1 cell enrichment and the expression of SREBF1. (M) Scatter plot showing the correlation between T helper 2 cell enrichment and the expression of SREBF1. (N) Scatter plot showing a positive correlation between B cell enrichment and the expression of SREBF1. \* $P < 0.05$ , \*\* $P < 0.01$ , \*\*\* $P < 0.001$ .

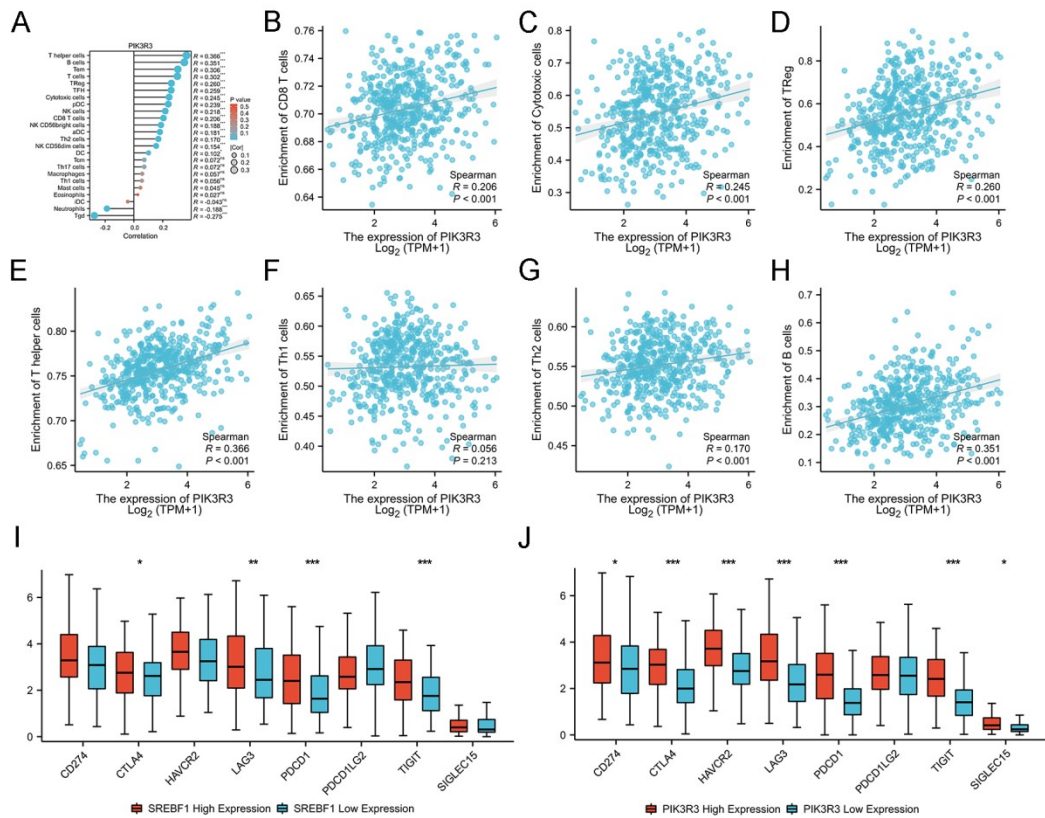


**Figure S8. The effect of SREBF1 on tumor immunity also depends on PIK3R3.** (A) Bubble plot representation showing the correlation between PIK3R3 and 24 immune cells in the HNSCC samples of the TCGA cohort. (B) Scatter plot showing a positive correlation between CD8 T cell enrichment and the expression of PIK3R3. (C) Scatter plot showing a positive correlation between cytotoxic cell enrichment and the expression of PIK3R3. (D) Scatter plot showing a positive correlation between regulatory T cell enrichment and the expression of PIK3R3. (E) Scatter plot showing a positive correlation between T helper cell enrichment and the expression of PIK3R3. (F) Scatter plot showing the correlation between T helper 1 cell enrichment and the expression of PIK3R3. (G) Scatter plot showing a positive correlation between T helper 2 cell enrichment and the expression of PIK3R3. (H) Scatter plot showing a positive correlation between B cell enrichment and the expression of PIK3R3. (I) Boxplot showing the expression of immune checkpoint proteins in the SREBF1 high- and low-expression groups. (J) Boxplot showing the expression of immune checkpoint proteins in the PIK3R3 high- and low-expression groups. \*P < 0.05, \*\*P < 0.01, \*\*\*P < 0.001.